MONITORING LAND COVER FIRES USING SPECTRAL INDICES AND SATELLITE DATA

Taha A.T. D. AlJawwadi
Assist. Prof.
Dep. Natu. Reso. and Engin. Scie.
Rem. Sen. Cen. Univ. Mosul
tars71@uomosul.edu.iq

Ayad A. Khalaf
Prof.
Dep. Soil andWat. Sci. Res.
Coll. Agric. Univ. Tikrit
aiad2017@tu.edu.iq

Abdalrahman R. Qubaa
Assist. Prof.
Dep. Image Proc. Rem. Sen. Cen.
Univ. Mosul
abdqubaa@uomosul.edu.iq

ABSTRACT

This study aimed to monitor and evaluate the impact of fires on the appearance of the land surface in open and flat agricultural areas using spectral indices and Landsat8 Operational Land Imagery (OLI) satellite images. A representative area, covering 250.34 km², was selected in Nineveh Governorate in Iraq lies between latitudes (43° 20′ 0″-43° 32′ 30″) N and longitude (36° 25′ 0″-36° 11′ 0″) E on June and July 2019 in order to determine the burned area on the land, and use the resulting spectral signature to generalize it to the rest of the study area. Data from the American Landsat satellite, GIS software, and spectral indicators for vegetation covers, such as the Normalized Difference Vegetation Index (NDVI), the Soil-Adjusted Vegetation Index (SAVI), and the Normalized Burning Ratio index (NBR), were used to extract the results. Then, the Land Surface Temperature index (LST) and the difference Normalized Burning Ratio index (dNBR) were used to measure the validity of the results and the severity of the fires, respectively. After using and performing corrective processing of the spectral indices, applying the three indices and determining the difference between them for a short period of time, it was possible to discover the areas of fires and the proportions of their effects. The NDVI results showed that the area affected by very severe degradation increased due to the fires to 39.29%, while the LST increased from 47.70 to 48.39 degree. The study concluded that the area of fire spread can be determined when there is a discrepancy in the pattern of spatial data that are close in date of capture and by using spectral indices.

Keywords: agricultural fires, agricultural indicators, surface temperature, remote sensing, GIS.

مراقبة حرائق الغطاء الارضي باستخدام المؤشرات الطيفية وبيانات الأقمار الاصطناعية

طه عبدالهادي الجوادي
قسم الموارد الطبيعية والعلوم الهندسية
مركز التحسس النائي
جامعة الموصل

اياد عبدالله خلف
قسم علوم التربة والموارد المائية
كلية الزراعة
جامعة تكريت

عبدالرحمن رمزي قبع
قسم المعالجة الرقمية
مركز التحسس النائي
جامعة الموصل

المستلخص

هدفت الدراسة إلى رصد وتقييم تأثير الحرائق على مظهر سطح الأرض في المناطق الزراعية المفتوحة والمسطحة باستخدام المؤشرات الطيفية وصور القمر الاصطناعي Landsat8 (OLI). ولقد تم اختيار منطقة ممثلة للدراسة بمساحة 250.3 كم^2، في الشهرين السادس والسابع 2019 في محافظة نينوى تقع ضمن خطوط العرض (43° 20′ 0″-43° 32′ 30″) شمالا وخطوط الطول (36° 11′ 0″-36° 25′ 0″) شرقا من أجل تحديد المنطقة المحروقة على الأرض واستخدام البصمة الطيفية الناتجة عنها لتعميمها على بقية منطقة الدراسة. تم استخدام بيانات القمر الاصطناعي الامريكي لاندسات وبرامجيات نظم المعلومات الجغرافية GIS واستخدام المؤشرات الطيفية الخاصة بالاغطية النباتية مثل مؤشر الفرق المعياري للغطاء النباتي NDVI ومؤشر الغطاء النباتي المعدل للتربة SAVI والمؤشر المعدل لنسبة الحرق NBR لاستخراج النتائج. وبعد إجراء المعالجة التصحيحية للمؤشرات الطيفية، وتطبيق معادلات المؤشرات الثلاثة وتحديد الفارق بينها، أمكن اكتشاف مساحات الحرائق ونسب تأثيراتها. ثم تم استخدام مؤشر درجة حرارة السطح LST والفرق للمؤشر المعدل لنسبة الحرق dNBR لقياس مدى صحة النتائج ومدى شدة الحرائق على التوالي. وأظهرت نتائج NDVI ان المساحة المتضررة بالتدهور الشديد بسبب الحرائق زادت إلى 39.29%، بينما زادت نسبة LST من 47.70 إلى 48.39 درجة. وخلصت الدراسة إلى أنه يمكن تحديد مساحة انتشار الحرائق عند وجود تباين في نمط البيانات الفضائية المكانية المتقاربة في تاريخ التقاطها باستخدام المؤشرات الطيفية.

الكلمات المفتاحية: الحرائق الزراعية، المؤشرات الزراعية، درجة حرارة السطح، التحسس النائي، نظم المعلومات الجغرافية.

Received:24 /10/2024, Accepted:9/2/2025, Published:December 2025

INTRODUCTION

The most important feature of the land surface in flat areas is the cultivation of field crops in addition to the presence of forest plants and others, which are considered pastoral lands. What the most affects these lands is the increase in the phenomenon of desertification as a result of unsustainable human activities such as overgrazing, urban expansion, poor irrigation systems, fires, deforestation, and others (13). Field crops are important sources of human life and a strategic storehouse for sustainable stability in the world (15). Some of them are considered among the most important fodder crops, which are considered the mainstay of livestock and sheep, and they have a major role in the agricultural economy, as livestock represent one of the basic food resources for humans. Wheat and barley are considered the first cereal crops on the list of field crops (25), and they are considered the main crops for most of the world's population, as they are considered the basic material for making bread and animal fodder. This importance is offset by their need for soil and plant management, which is relatively easier compared to other crops. These crops go through several different growth stages (1, 3). Each of these stages-like other crops-is accompanied by some risks, diseases and harsh environmental conditions, through which farmers must know what these risks are and how to contain them and be aware of them in advance. If these symptoms can be controlled in the crop's life cycle, the vast areas in which the crop is grown, especially crops that depend on rain-fed agriculture, make these risks a cause in quantities with great economic potential (2). Perhaps the maturity period of wheat and barley crops, which represents the complete drying of the plant after expelling the ears, is one of the most sensitive and dangerous periods in the life cycle of the crop (3), as it is the period in which the plant is parched and has a high plant density and in very hot seasons, especially in dry and semi-arid areas, which makes it susceptible to rapidly spreading fires, especially since the degree of burning of plants at this stage will be low. Fires in agricultural fields affect the availability of nitrogen in the soil, and it is known that it is a decisive factor for soil fertility. The causes of fires that can be monitored on the surface of the Earth are many, some of which are due to burning open fields, which is a method widely used to remove crop residues from agricultural lands (15). Or farmers' mistakes during harvesting, and cigarette butts that are discarded negligently, as well as agricultural harvesting machines that may be the cause of the combustion process because the exhausts of these machines are hot and may send out small fiery masses or sparks that may not be noticed by those in charge of harvesting, in addition to the overlapping of these vast fields, and other fires caused by nature, such as lightning. Its proximity to barren lands covered by dry and dense forests, which have the same causes of burning wheat and barley crops. As well as the causes that may be intended for individual or social disputes and conflicts. The extent of fires, the speed and spread of their damage over the land area as a result of their impact and the surrounding areas, and their risks cannot be easily known, so there was a need for remote sensing and to take advantage of the special development and the enormous change in temporal, spatial and spectral characteristics. Remote sensing satellites have the ability to quickly identify fire locations by analyzing satellite observations of the same area and over multiple time periods covering fire events for that period (26). High temporal resolution satellites such as EOS/MODIS and NOAA/AVHRR are able to accurately identify burned areas and their temporal changes, although they have low spatial resolution, while medium resolution satellites such as the Landsat series are able to accurately detect burned areas with spatial resolution (30 meters). One of the most important Earth observation satellites for this purpose is the latest Landsat generation, Landsat 8, whose OLI sensor can capture multispectral images covering several spectral bands of wavelengths, where the near-infrared (NIR) range (0.85-0.88 μm) is often used. Two shortwave infrared (SWIR) bands (1.57-1.65 μm and 2.11-2.29 μm) were used to identify burned areas. Vegetation indices are critical for collecting significant information about plant health, density, and distribution from remotely sensed data (19). EVI, GDVI2, NDSI, SI, and OSAVI, each with its spectral sensitivity, provide information about vegetation status and stress variables (5). These indicators are useful in identifying land cover types, monitoring vegetation behavior, and analyzing environmental changes (17). Also the vegetation indicators were used for classification and monitoring agricultural lands (4,24). For discrimination purposes, the following criteria and guidelines were used: The Normalized Difference Vegetation Index (NDVI) to indicate the intensity of vegetation in an area, as well as the Soil Adjusted Vegetation Index (SAVI) which is a factor-

corrected soil in the NDVI formula (21). Land surface temperature (LST) is defined as the thermal emission from the surface, including the tops of canopies in vegetated areas and bare soils. It is a crucial factor in atmospheric sciences, reflecting surface, atmosphere interactions and energy fluxes. LST serves as a good index of energy balance at the Earth's surface and provides important information about physical characteristics and climate, influencing various environmental processes. Many researchers have studied LST and vegetation indices (18). LST is also a major index for crop or forest fires. Fire-induced environmental changes resulted in a variance in LST values (7). The aim of this research is the possibility of identifying and estimating burned areas in addition to the Earth's surface temperature using spectral indicators from remote sensing data and geographic information systems. This approach enhances the accuracy of fire assessments, enabling more effective management and mitigation strategies for agricultural lands affected by fire.

MATERIALS AND METHODS

Study area: A study area was chosen to represent lands. It has a ground cover that is susceptible to burning quickly and can be easily monitored in satellite data, such as the wheat and barley crops in Nineveh Governorate, located east of the city of Mosul, the center of the governorate, which is located between two latitudes (43˚ 20′ 0) - (43˚ 32). ′ 30) E and longitude (36˚ 25′ 0) - (36˚ 11′ 0). The study area, spanning 250.34 km², included a representative field test site selected to directly assess the burned area. This enabled the generalization of the observed spectral signature from the known site to the entire study region. This area, called the Nineveh Plain, is a rain-fed wheat and barley growing area and is considered one of the best areas in Nineveh Governorate in terms of land settlement, soil type and lack of rain-fed agriculture due to the semi-arid climate according to the Köppen classification of climate zones in Nineveh Governorate. Figure (1) shows the study area and the classification of the soils of the study area according to the Food and Agriculture Organization within the classification of the Vertisol class, which is characterized by a high percentage of clay and $CaCO_3$, according to Table.1 (13,16).

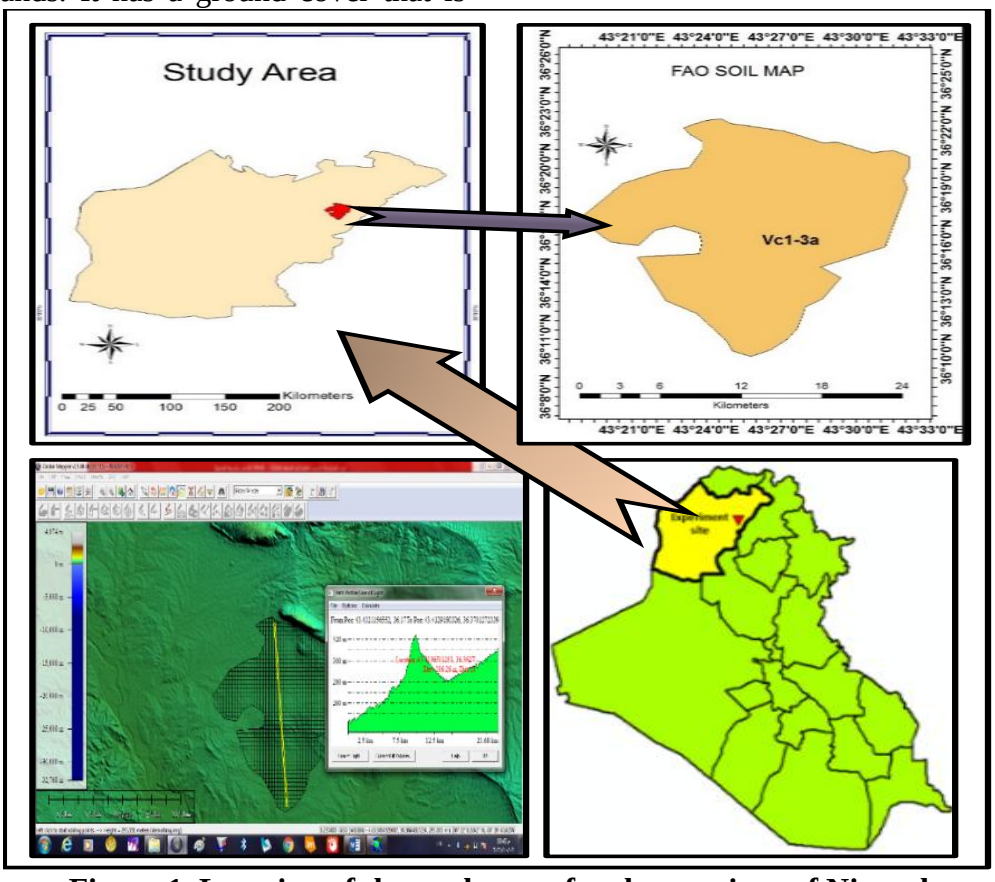

Figure 1. Location of the study area for the province of Nineveh

Table 1. Soil properties in the study area

Properties	Unit	Surface (0-30 cm)	Subsurface (30-60 cm)
Sand		16	15
Silt	(%)	29	28
Clay		55	57
Bulk Density	(µg/m³)	1.65	1.76
Gravel Content	(%)	4	5
Organic Carbon		0.75	0.45
pH		7.6	8.1
CEC_{Clay}	(cmol/kg)	75	73
CEC_{Soil}		44	43
BS%		100	100
$CaCO_3$	(%)	2.5	3.9
ESP		1	3
Salinity (Ece)	(dS/m)	0.2	0.3

Remote Sensing Data

Satellite image: A Landsat 8 OLI satellite images was chosen. Two shortwave infrared (SWIR) bands (1.57-1.65 µm and 2.11-2.29 µm) were used to identify burned areas on (9-7-2019), and this period is very close to the period when the true fire occurred. Another image was chosen on (23-06-2019), which is the period before the fires broke out. The area through field detection, as shown in Figure (2). ArcGIS was used to process and display the data (12).

Image Processing: Initially the Landsat 8 OLI- Operational Landsat Imager images were converted from DNs to reflectivity using the equations published by USGS Landsat 8. Image processing of band was conducted base on equation 1 and 2, as shown below:

$$P_{\lambda}' = M\rho \times Q_{cal} + A_{\rho} \quad \text{..... (1)}$$

Where: ρλ'= TOA (Top of Atmosphere) planetary reflectance, without solar angle correction.

Mρ= Band-specific multiplicative rescaling factor from the metadata (REFLECTANCE MULT BAND x, where x is the band number);

Q_{cal}= Quantized and calibrated standard product pixel values (DNs);

A_{ρ}= Band-specific additive rescaling factor from the metadata.

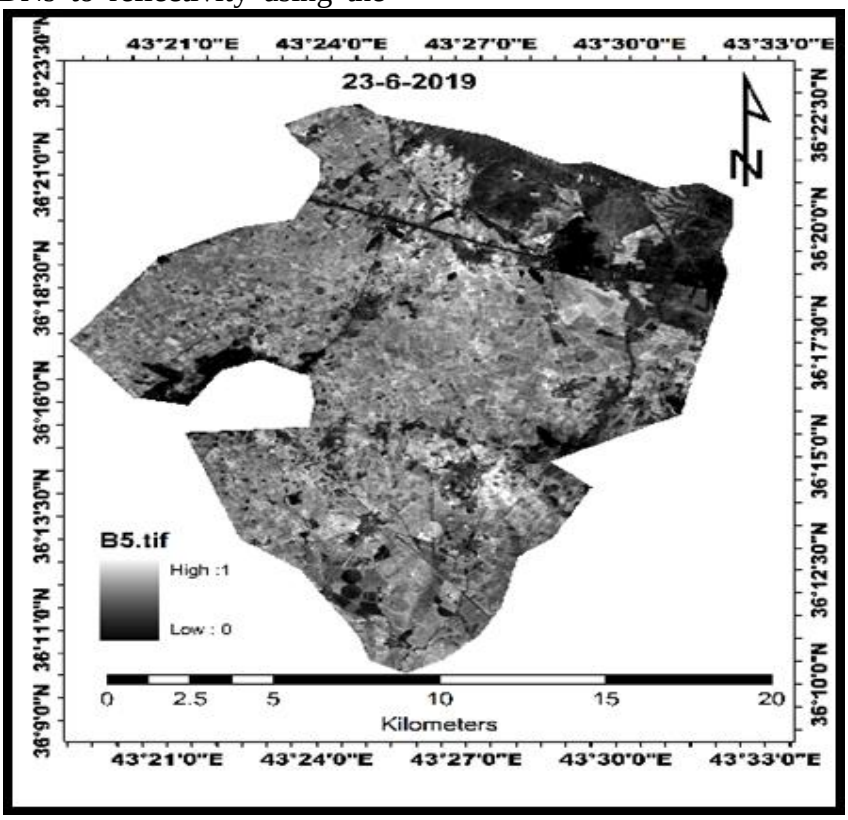

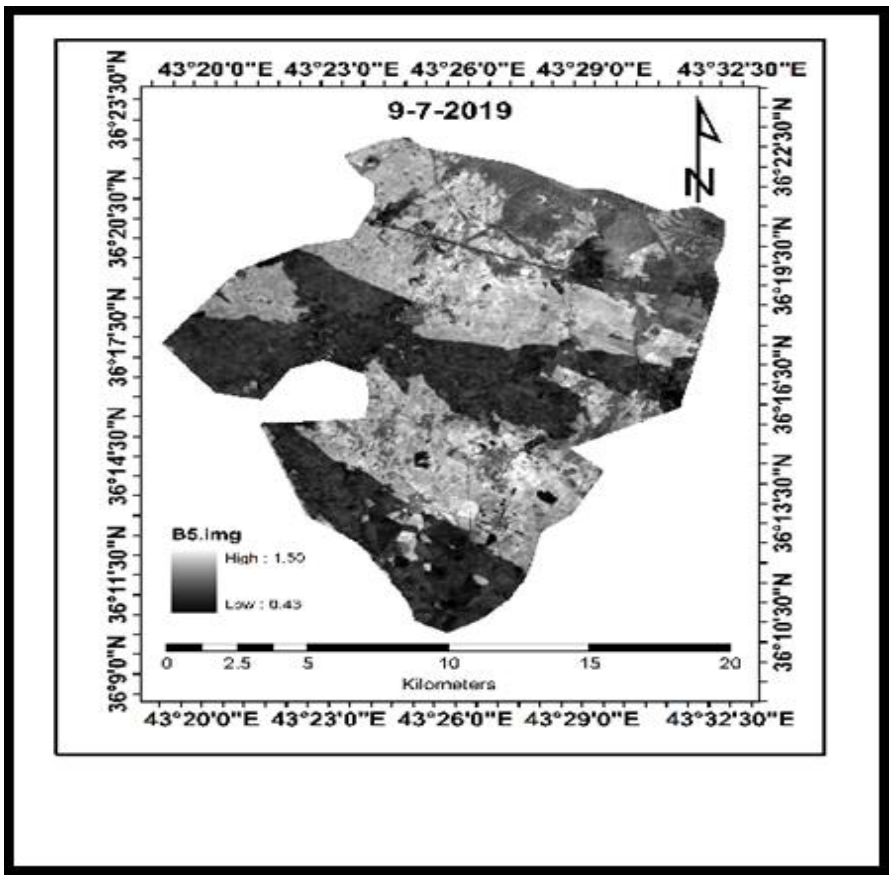

Figure 2. Satellite image of study area in two periods

Then, TOA reflectance with a correction for the sun angle was calculated using the Eq. (2):

$$R_\lambda = \frac{\rho\lambda'}{sin\ \theta_{SE}} \quad \ldots\ldots\ldots\ldots\ldots\ldots\ldots\ldots\ldots\ldots (2)$$

Where: Rλ= TOA planetary reflectance; θ_{SE}= Local sun elevation angle; which provide in degrees in the metadata (SUN_ELEVATION). Both equations were applied using ERDAS software.

Spectral Indices: For the purposes of discrimination, the following indicators and evidence have been used:

Normalized Difference Vegetation Index (NDVI): which typically captures chlorophyll concentration to characterize the state of plant health, and to indicate the intensity of vegetative growth in an area. It is used to track forest regrowth and restoration to a healthy state, as it is sensitive to changes in vegetation and has been shown to accurately detect leaf disturbances ending in forest disturbances (6). It is easily computed using the reflection image display in the red and infrared bands, and hence Landsat 8 OLI (Operational Land Imager) images in spectrum bands 4 and band 5, it can be used to compute NDVI, allowing to detect the state of vegetation areas (forests, grasses, groves, ...) as well as to characterize water (oceans, seas, lakes, rivers, ...) and soil (rocks, buildings Roads (27). TOA transformation of the original data was used to calculated of NDVI as in Eq. (3).

NDVI = (ρBand 5 – ρBand 4) / (ρBand 5 + ρBand 4) ……. (3)

Where: B5 = near infrared band; B4=Red band

Soil Adjusted Vegetation Index (SAVI): It incorporates a soil correction factor into the NDVI equation, whereby SAVI is applied in the NDVI correction of the effect of soil brightness in areas with low vegetation cover (14). Eq. (4)

SAVI = ((ρBand 5 – ρBand 4) / (ρBand 5 + ρBand 4 + 0.5)) * (1.5) ..(4)

Where, **ρBand 5** = Surface Reflectance of near infrared band; **ρBand 4**= Surface Reflectance of Red band, and L= value may be applied to a wide range in vegetation densities **(0.5, 1.0, 1.5)**

Normalize Burn Ratio –NBR: It is the ratio between near infrared with SWIR short infrared rays confined within range (2.08-2.35 μm), to determine the burning areas after the fire and to provide a quantitative measure of the burning intensity (22) Eq. (5)

NBR = (ρBand 5 – ρBand 7) / (ρBand 5 + ρBand 7) ……..…… (5)

Where ρBand 5 = Surface Reflectance of near infrared band and **ρBand 7** = Surface Reflectance of SWIR-2: Shortwave Infrared 2

Differenced Normalized Burn Ratio (dNBR): It is measured change in NBR, and related in size to the environmental change induced by the fire in terms of the severity of fire impact on pre-existing plant communities (22). As well as, to isolate the burned areas from the unburned and to provide a quantitative measure of change dNBR calculated by subtracted post-burn NBR dataset from pre-burn NBR dataset according to equation (5) as in Eq. 6 (8).

$$dNBR = NBR_{prefire} - NBR_{postfire} \ldots\ldots\ (6)$$

Where, NBR= Normalized Burn Ratio before fire and post fire.

The intensity of the fire in the area can be known through the dNBR values according to Table (2) (29).

Table 2. Severity of the burn according to dNBR values

Burn Severity	dNBR
Unburnt	-0.10 – 0.10
Low severity	0.10 - 0.27
Medium severity	0.27 - 0.44
High severity	0.44 - 0.66
Very high severity	> 0.66

Land Surfaces Temperature (LST): is an important variable in the physics of terrestrial - surface processes that controls heat and water flow at the interface between the Earth's surface and the atmosphere. The LST is an important parameter in the interaction between the Earth's surface and the atmosphere (9,20,28). Remote sensing space data provides the only possible way to acquire high-precision LST in the spatial and temporal domain worldwide. The land surface temperature was used according to steps as following:

$$L\lambda = ML * Qcal + AL \quad \ldots\ldots\ (7)$$

Lλ=Spectral radiance(W/(m2*sr*µm)) .. (8)

ML: Radiance multiplicative scaling factor for the band RADIANCE_MULT_BAND_n from the metadata)

AL = Radiance additive scaling factor for the band (RADIANCE_ADD_BAND_n from the metadata).

Qcal = Level 1 pixel value in DN

$$TB = \left(\frac{K2}{LN\left(\frac{K1}{L\lambda}+1\right)} \right) - 273.15 \ldots\ldots\ldots\ldots (9)$$

TB=Top of atmosphere brightness temperature (C°) where

K1, K2: Band-specific thermal conversion constant from the metadata (K1_CONSTANT_BAND 10, where x is the thermal band number) Band-specific thermal conversion constant from the metadata (K2_CONSTANT_BAND_x, where x is the thermal band number)**.**

Lλ= TOA spectral radiance (Watts/ (m2 * srad * µm))

$$Pv = \left[\frac{NDVI - MinNDVI}{MaxNDVI - MinNDVI}\right]^2 \ldots\ldots\ldots\ldots\ldots (10)$$

Pv: Vegetation proportion.

$$\varepsilon = 0.004 \times Pv + 0.986 \quad \ldots\ldots\ldots\ldots (11)$$

ε: Emissivity

$$LST = \frac{TB}{1 + (L\lambda \times \frac{TB}{14380}) \times LN(\varepsilon)} \quad \ldots\ldots\ldots (12)$$

RESULTS AND DISCUSSION

Table (3) shows the selected criteria, based on which the area's degradation is divided into four categories starting with (very sever degradation) and ending with (slightly degradation) (23,28). The indicator NDVI shows amounted to about (16.98%) from the total area affected by degradation very severely, which increased suddenly in about sixteen days to (39.29%). This percentage cannot increase in this short period in the usual environmental changes unless there is an intervention of a large human factor or the effect of the fires that actually occurred in that period, and there was actually a fire according to the field inspection conducted by the researchers during that period, as shown in Figure (3).

Table 3. Values and percentages of some selected indicator in the study.

DEGRADATION DEGREE	NDVI	%	SAVI	%	NBR	%
			23/6/2019			
very sever degradation	4250.43	16.98	3174.66	12.68	3825.00	15.3
sever degradation	12630.24	50.46	11839.32	47.30	9237.96	36.9
moderate degradation	7527.69	30.07	9463.95	37.81	8248.59	33.0
slightly degradation	625.14	2.50	555.57	2.22	3721.68	14.9
			09/07/2019			
very sever degradation	9835.74	39.29	9718.65	38.83	9371.97	37.5
sever degradation	3511.44	14.03	3773.25	15.07	5598.81	22.4
moderate degradation	7799.49	31.16	6083.91	24.31	5781.96	23.1
slightly degradation	3884.40	15.52	5455.35	21.79	4272.03	17.1

***The degree of degradation are classified according to (28)**

Whereas, sever degradation decreased from 50.46% in the first image to 14.03% in the second image, and this difference does not explain the improvement in the condition of the region, but rather indicates the transfer of a large proportion of S.D. to V.S.D. Moderate degradation was almost constant for the semi-arid regions, in which distances between the plants were not affected by the fires greatly when compared to field crops planted with densities and completely dry, and this explains the almost constant proportions. While slightly degradation percentage increase explained by the restoration of some plants to their vegetative growth under sprinkler irrigation areas. These interpretations do not differ much with respect to the results of the SAVI index value, as they were close to the results of the NDVI index value, as shown in Figure (4). For the purpose of increasing the interpretation of the region further, a comparison of NDVI index values for 560 pixels chosen for the same area for both images, which shown, as in Figure (5), the general decline in the NDVI values for the region in the second image. According to Table (4), (11), this decrease is explained area transformation into barren land or plant remains The NDVI values for most points in the second image ranged between 0.140 and 0.025

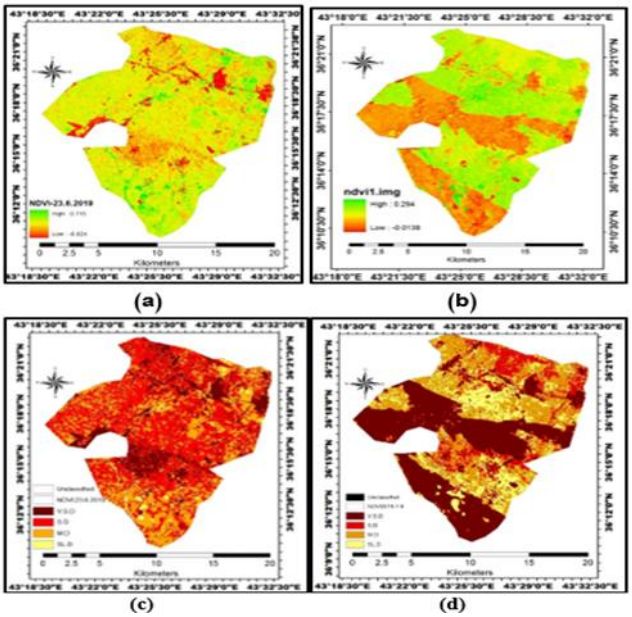

Figure 3. NDVI classification of the study area: a. NDVI on 23-6-2019 b. NDVI on 9-7-2019 c. Classification of four categories of degradation on 23-6-2019 and d. Classification of four categories of degradation on 9-7-2019

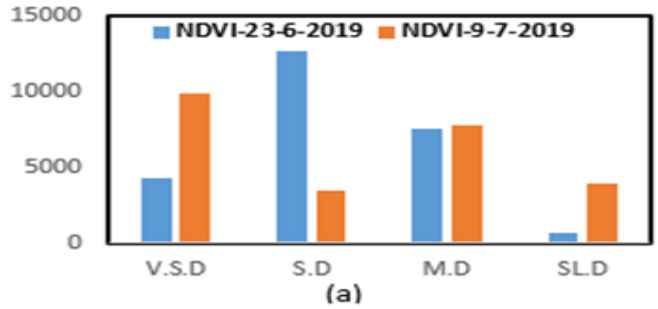

(a)

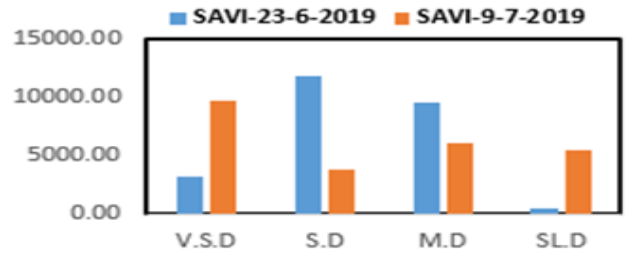

(b)

Figure 4. NDVI and SAVI indices of study area: (a) NDVI (b) SAVI

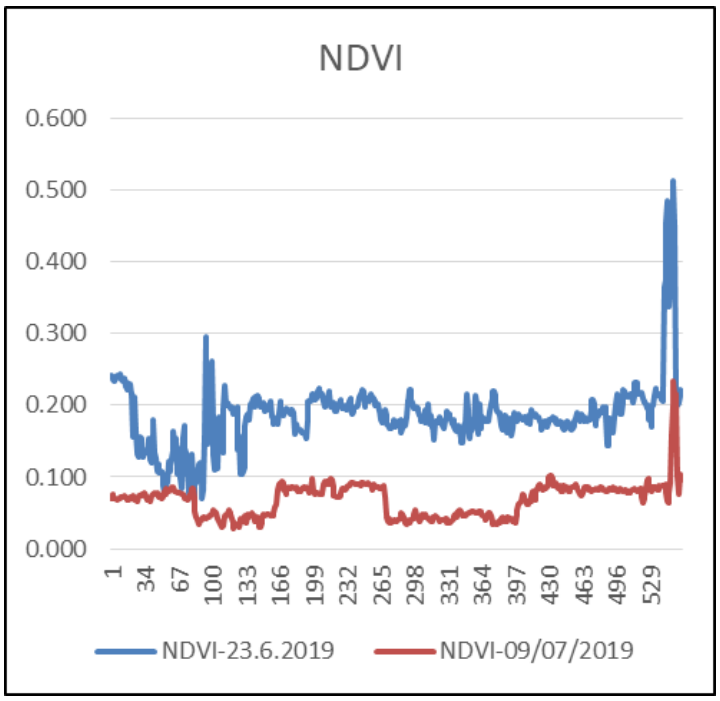

Figure 5. NDVI values for selected points

Table 4. Indicative values of NDVI index in different land cover types

Type of Land Cover	NDVI (scale from -1 to 1)
Thick Vegetation	0.500<=NDVI<=1
Medium Vegetation	0.140<=NDVI<0.500
Scarce Vegetation	0.090<=NDVI<0.140
Bare ground	0.025<=NDVI<0.090
Clouds	0.002<=NDVI<0.025
Ice and snow	-0.046<=NDVI<0.002
Water	-1<=NDVI<-0.046

For distinguishing whether these areas were actually burned, and because not all changes in land cover can be caused by fires (28), the NBR index and dNBR were used, which were calculated according to equation (5). As a result, most of the area was burned with varying severity. The dNBR values for unburned areas are close to zero, while the values for burned areas are positive or strongly negative, depending on whether the fire disturbs or actually enhances the productivity at the site (22). As shown in Figure (6).

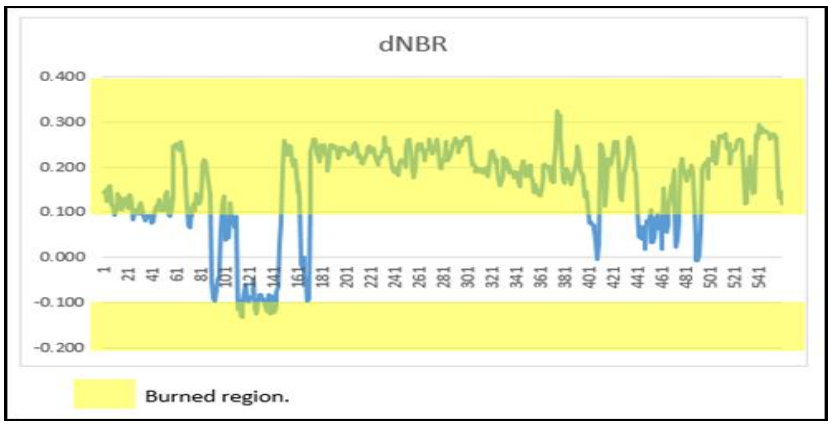

Figure 6. dNBR values for selected points

Table (5) shows the values of the parameters used to calculate the land surface temperature index (LST), according to equation (11). The results showed that the average and standard deviation of the LST were (47.70 and 1.21) respectively before the fire, while the LST values for the average and standard deviation after the fire were (48.39 and 2.59) respectively, as it is noted from the values that there was a noticeable increase in the temperature of the Earth's surface, as shown by previous articles (11), which is due to two reasons, one of which is the impact of the study area was affected by the heat of the fire, and secondly, the surface of the Earth gained more heat due to the presence of black plant residues resulting from the fire, which increased the absorption of sunlight and thus raised the temperature of the Earth's surface, as shown in Figure (7).

Table 5. Parameters values used to calculate land surface temperature index

Statis.	min	max	mean	Std. deviation
		2019/06/23		
Ly	11.05	14.06	12.83	0.2
TB	36.66	54.88	47.68	1.21
PV	0.00	1.00	0.08	0.03
e	0.99	0.99	0.99	0.00
LST	36.67	54.91	47.70	1.21
		2019/07/09		
Ly	10.69	14.25	12.95	0.44
TB	34.27	55.97	48.37	2.59
PV	0.00	1.00	2.25	0.04
e	0.99	0.99	0.99	0.00
LST	34.28	56.00	48.39	2.59

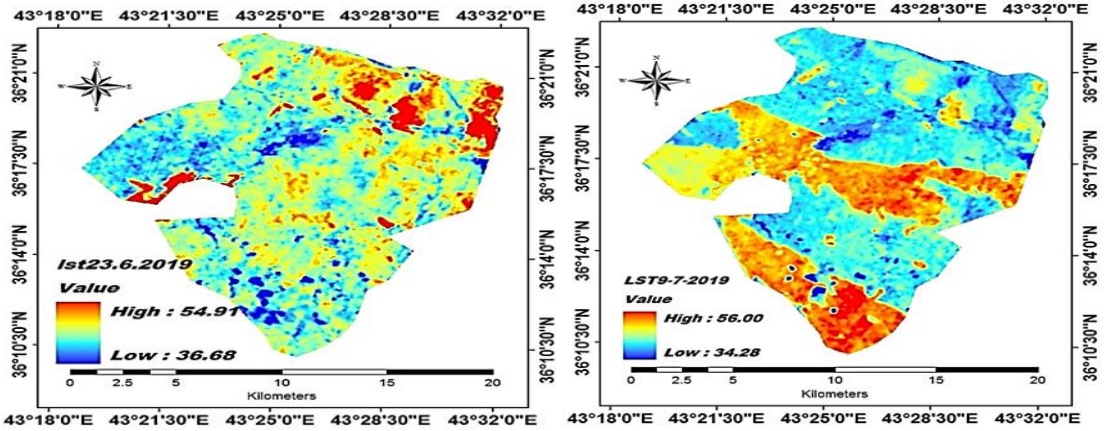

(a) **(b)**

Figure 7. LST values for Study Area. (a) 23-6-2019 (b) 9-7-2019

CONCLUSION

Spectral evidence based on satellite data has been used in this study to detect and assess burned agricultural lands. A number of specialized indicators are used to isolate the condition of healthy vegetation, such as NDVI, and the effects of soil with vegetation, such as SAVI, in addition to more specialized evidence. On fire, such as NBR, which not only diagnoses the burned area but also allows

diagnosis of fire severity through dNBR. The ground surface temperature (LST) index was also used as evidence that the fire had actually occurred. The NDVI results showed that the area affected by severe deterioration due to fires increased to 39.29%, while the LST increased from 47.70 to 48.39 degrees. The study concluded that agricultural indices can be used to detect the location and severity of fires. This approach enhances the accuracy of fire assessments, enabling more effective management and mitigation strategies for agricultural lands affected by fire.

CONFLICT OF INTEREST

The authors declare that they have no conflicts of interest.

DECLARATION OF FUND

The authors declare that they have not received a fund.

REFERENCES

1. Anbar, A. R., and A. I. Hamad 2025. Evaluation of land suitability for irrigated wheat cultivation using two different methods in northern Ali Al-Gharbi district. Iraqi Journal of Agricultural Sciences, 56(Special), 148-160. https://doi.org/10.36103/ty99hy27

2. Antonello, B, F. Terribile, J. and Bouma, 2019. Refining physical aspects of soil quality and soil health when exploring the effects of soil degradation and climate change on biomass production: An Italian case study. Soil, 5(1), 1-14. https://doi.org/10.5194/soil-5-1-2019, 2019.

3. Ali; B., and A. Gholizadeh, 2016. Modeling land suitability evaluation for wheat production by parametric and TOPSIS approaches using GIS, northeast of Iran. Modeling Earth Systems and Environment, 2(3), 126. https://doi.org/10.1007/s40808-016-0177-8

4. Akram, A. A. and A. I. Hamad 2024. Spatial variability of the heat emitted from the land surface in determining the characteristics of desert soils in Al-Samawah desert using "GIS". Iraqi Journal of Agricultural Sciences, 55(5), 1637-1649. https://doi.org/10.36103/03zbrj03

5. Akrawi, S., and K. Alkhaled 2024. Monitoring land cover variation using some spectral indicators in Akre region based on geospatial techniques. Mesopotamia Journal of Agriculture, 52(2), 130-145. doi: 10.33899/mja.2024.145686.133014

6. Al-Arazah A. A., K. Naser, and A. I. Hamad 2021. Use of geographic information systems in production of salt maps prevailing in Al-Maimuna project in southern Iraq. International Journal of Agricultural and Statistical Sciences, 17, 1851. https://connectjournals.com/03899.2021.17.1851

7. Anupam, P., A. Mondal, S. Guha, P. K. Upadhyay, Rashmi, and S. Kundu, 2024. Comparing the seasonal relationship of land surface temperature with vegetation indices and other land surface indices. Geology, Ecology, and Landscapes, 1-17. https://doi.org/10.1080/24749508.2024.2392391

8. Athanasakis, G., P. Emmanouil and C. Andromachi 2018. High-Resolution earth observation data and spatial analysis for burn severity evaluation and post-fire effects assessment in the Island of Chios, Greece. SPIE Remote Sensing. https://doi.org/10.1117/12.2278271.

9. Chen X., et al. 2014. Retrieving China's surface soil moisture and land surface temperature using AMSR-E brightness temperatures. Remote Sensing Letters 5(7):662-71. https://doi.org/10.1080/2150704X.2014.960610.

10. Dregne, H. E, and N. T. Nan-ting 1992. Global desertification and costs. Degradation and Restoration of Arid Lands: 289. http://www.ciesin.org/docs/002-186/002-186.html.

11. Eva, H. and E. F. Lambin, 2000. Fires and land-cover change in the tropics: A remote sensing analysis at the landscape scale. Journal of Biogeography, 27(3), 765–776. http://www.jstor.org/stable/2656223

12. FAO, Food and Agriculture Organization of the United Nations 2021. World reference base for soil resources 2014. https://openknowledge.fao.org/server/api/core/bitstreams/bcdecec7-f45f-4dc5-beb1-97022d29fab4/content

13. Hadeel, A. S., M. T. Jabbar, and X. Chen, 2010. Application of remote sensing and GIS in the study of environmental sensitivity to desertification: a case study in Basrah Province, southern part of Iraq. *Applied*

Geomatics, *2*(3), 101-112. https://doi.org/10.1007/s12518-010-0024-y
14. Hislop, S., S. Jones, M. A. S. Hadeel, M. T. Jabbar, and X. Chen, 2010. Application of remote sensing and GIS in the study of environmental sensitivity to desertification: a case study in Basrah Province, southern part of Iraq. Applied Geomatics, 2(3), 101-112.
15. Hummadi, A. H. and Khalaf A. 2024. Temporal and spatial variation of agricultural drought and desertification using spectral indices in Salah Al-Din governorate. Tikrit Journal for Agricultural Sciences, 24(1), 206-222.doi: 10.25130/tjas.24.1.17
16. Junaidi, S. N. et al. 2021. Analysis of the relationship between forest fire and land surface temperature using Landsat 8 OLI/TIRS imagery. IOP Conference Series: Earth and Environmental Science 767(1). https://dx.doi.org/10.1088/1755-1315/767/1/012005
17. Kadhim, M. M. 2018. Monitoring land cover change using remote sensing and GIS techniques: a case study of Al-Dalmaj marsh, Iraq. Journal of Engineering, 24(9), 96-108. https://doi.org/10.31026/j.eng.2018.09.07
18. Khalaf, A. and A. Hummadi 2023. Time series analysis of drought indices for monitoring desertification and land degradation. Iraqi National Journal of Earth Science, 23(2). https://doi.org/10.33899/earth.2023.139660.1068
19. Khalaf, A. B. 2019. Use the NDVI index to classify the land covers of the city of Baquba and its outskirts. Mesopotamia Journal of Agriculture.(47)I. https://www.iasj.net/iasj/article/188410
20. Kumar, P., K. Binay and R. Meenu 2013. An efficient hybrid classification approach for land use/land cover analysis in a semi-desert area using ETM+ and LISS-III sensor." IEEE Sensors Journal 13(6): 2161–65. doi:10.1109/JSEN.2013.2251462
21. Krenz, J., P. Greenwood, N. J. and Kuhn, 2019. Soil degradation mapping in drylands using Unmanned Aerial Vehicle (UAV) data. Soil Systems, 3(2), 33. https://doi.org/10.3390/soilsystems3020033
22. Lutes, C. D. 2006. Fire effects monitoring and inventory system. U.S. Department of Agriculture, Forest Service, Rocky Mountain Research Station. http://dx.doi.org/10.2737/RMRS-GTR-164
23. Pimentel, D., et al. 1995. Environmental and economic costs of soil erosion and conservation benefits. Science, 267(5201), 1117–1123. http://www.jstor.org/stable/2886079
24. Pajares, G. 2015. Overview and current status of remote sensing applications based on unmanned aerial vehicles (UAVs). Photogrammetric Engineering and Remote Sensing, 81(4), 281-330. https://doi.org/10.14358/PERS.81.4.281
25. Sallam, A., A. M. Alqudah, M. F. Dawood, P. S. Baenziger, and A. Börner, 2019. Drought stress tolerance in wheat and barley: advances in physiology, breeding and genetics research. International journal of molecular sciences, 20(13), 3137. https://doi.org/10.3390/ijms20133137
26. San-Miguel-Ayanz, J., and N. Ravail, 2005. Active fire detection for fire emergency management: Potential and limitations for the operational use of remote sensing. Natural Hazards, 35(3), 361-376. https://doi.org/10.1007/s11069-004-1797-2
27. Xie, Q. et al. 2015. Evaluating the potential of vegetation indices for winter wheat LAI estimation under different fertilization and water conditions. Advanced Space Research 56: 2365–73. https://doi.org/10.1016/j.asr.2015.09.022.
28. Zhou, F et al. 2018. A practical two-stage algorithm for retrieving land surface temperature from AMSR-E Data-A case study over China." IEEE Journal of Selected Topics in Applied Earth Observations and Remote Sensing 11(6): 1939–48. doi: 10.1109/JSTARS.2018.2799552
29. Zhu, Z. et al. 2020. Evaluate sensitivities of burn-severity mapping algorithms for different ecosystems. U.S. Forest Service. Fire effects information system. https://www.frames.gov/catalog/16184